Volume 1 | Number 1 | Jan 2013 | Pages 1–100

Journal of
Materials Chemistry A

Materials for energy and sustainability
www.rsc.org/materialsA

ROYAL SOCIETY
OF CHEMISTRY

ROYAL SOCIETY
OF CHEMISTRY

www.rsc.org/materialsA

Remarkable Gas Adsorption by Carbonized Nitrogen-Rich Hypercrosslinked Porous Organic Polymers

Xiao Yang, Miao Yu, Yang Zhao, Chong Zhang, Xiaoyan Wang, Jia-Xing Jiang*

A series of carbonized materials was obtained using nitrogen-rich hypercrosslinked porous organic polymer as the precursor by high-temperature treatment with/without potassium hydroxide activation. Compared with the carbon materials without potassium hydroxide activation, the potassium hydroxide activated carbons show higher surface areas and enhanced gas uptake abilities. The activated carbon material of FCDTPA-K-700 exhibits a high surface area of 2065 m^2 g^{-1} and an exceptionally high carbon dioxide uptake up to 6.51 mmol
10 g^{-1} (1.13 bar / 273 K) with a hydrogen uptake ability of 2.61 wt % (1.13 bar / 77 K). Moreover, the methane storage ability of 2.36 mmol g^{-1} (1.13 bar / 273 K) by FCDTPA-K-700 is also comparable to that of the most porous materials reported. Given the high surface areas, the outstanding gas sorption performances, and the facile preparation strategy, these novel carbon materials are very promising for industrial applications such as carbon dioxide capture and high-density clean energy storage.

Introduction

15 The increasing anthropogenic emission of CO_2 produced from the rapid consumption of fossil fuels is known to be responsible for the global climate change and some environment issues. The carbon dioxide capture and utilizing clean energy such as hydrogen, therefore, are potential strategies to solve these issues.[1]
20 Many strategies have been developed to capture of carbon dioxide and most works are focused on the porous solid adsorbents,[2-5] which physisorb CO_2 molecules through relatively weak van der Waals forces making the regeneration of the materials energy efficient. To date, a range of microporous solid
25 adsorbents have been proposed for capture of carbon dioxide including zeolites,[6] metal-organic frameworks (MOFs),[7] porous organic molecules (POMs),[8, 9] microporous organic polymers (MOPs),[10, 11] and microporous carbons.[12, 13]

Microporous carbon materials show some advantages such
30 as high surface area, robust chemical and thermal stability, lightweight, fast kinetics, diverse availability, and facile preparation strategies.[12] This could make microporous carbons strong candidates for carbon capture and clean energy storage, and have been the subject of intense recent interest. For example,
35 the YSN-1$_{400\,°C}$ carbonized from the spirobifluorene-based porous organic polymer showed a hydrogen uptake ability of 2.6 wt% at 1 bar and 77 K,[14] the MOF-derived hierarchically porous carbon, MDC-1, showed an exceptional hydrogen uptake capacity of 3.25 wt% at 1 bar and 77 K,[15] the carbonized porous aromatic
40 framework, PAF-1-450, could absorb 4.5 mmol g^{-1} CO_2 at 1 bar and 273 K,[16] the KOH-activated carbonized PAF-1 derivative, K-PAF-1-600, exhibited an exceptional CO_2 uptake capacity of 7.2 mmol g^{-1} at 1 bar and 273 K,[17] and the PAF-1/C-900 produced from PAF-1 with extra carbon source could adsorb 4.1 mmol g^{-1}
45 CO_2 at 1 bar and 295 K.[18] It has been also suggested that the

incorporation of heteroatoms such as nitrogen into the carbon nanomaterials could enhance the CO_2 and energy-storage properties.[19, 20] For example, N-doped template carbon of N-TC-EMC from zeolite EMC-2, possessed remarkable CO_2 capacity of
50 4.00 mmol g^{-1} at 1 bar and 298 K,[21] the NPC-650 carbonized from porous polyimine demonstrated the CO_2 capture performance of 5.26 mmol g^{-1} at 1 bar and 273 K,[22] the nitrogen-decorated nanoporous carbon of NC900 from N-rich ZIF-8 exhibited the CO_2 adsorption capacity of 5.1 mmol g^{-1} at 1 bar
55 and 273 K,[23] and the nitrogen enriched porous carbon spheres produced from the sol-gel method could absorb 6.2 mmol g^{-1} CO_2 at 1 bar and 273 K.[24] These results demonstrated that such N-decorated carbon materials have great potential to increase the CO_2 capture capacity.

60 In this work, a nitrogen-rich hypercrosslinked porous organic polymer network was designed and synthesized. A series of carbonized materials based on the precursor, therefore, has been obtained by high-temperature treatment with/without potassium hydroxide activation. As potassium hydroxide has been
65 used as an efficient chemical agent to produce highly porous carbon materials,[17, 25] we expect that the potassium hydroxide activation during the carbonization could substantially increase the surface area of the resulting carbon materials and, on the other hand, the incorporation of nitrogen atom into the carbonized
70 materials could enhance the binding affinity between the adsorbent and CO_2 molecules which results in the increase of CO_2 capture capacity.

Experimental section

Materials

75 Triphenylamine (TPA) was purchased from Alfa. Formaldehyde dimethyl acetal (FDA), anhydrous $FeCl_3$, 1,2-dichloroethane

(DCE) and other chemicals were obtained from J&K Scientific Ltd. All chemicals were used as received. The monomer of *N, N, N′, N′*-tetraphenylbiphenyl-4,4′-diamine (DTPA) was synthesized according to the literatures.[26, 27]

Synthesis of the nitrogen-rich hypercrosslinked porous polymer (FCDTPA)

To the mixture of DTPA (0.488 g, 1.0 mmol) and FDA (0.304 g, 4.0 mmol) in 20 mL 1,2-dichloroethane, anhydrous FeCl$_3$ (0.649 g, 4.0 mmol) was added at room temperature. The mixture was heated to 80 °C and stirred for 24 h under a nitrogen atmosphere. The mixture was then cooled down to room temperature and the precipitated network polymer was filtered and washed with methanol, distilled water, dichloromethane and acetone successively, until the filtrate was nearly colorless. The further purification of the polymer network was carried out by Soxhlet extraction from methanol for 48 h. The product was dried in vacuum for 24 h at 70 °C to give deep green powder (Yield: 460 mg, 95.04 %). Elemental combustion analysis (%) Calcd. for (C$_{40}$H$_{32}$N$_2$)$_n$: C 88.89, H 5.93, N 5.18; Found: C 89.29, H 5.81, N 4.90.

Synthesis of the carbon materials by directly heating treatment

The precursor of FCDTPA was heated directly to the target temperatures of 500, 700 and 900 °C with a heating rate of 2 °C min^{-1} in a nickel crucible placed within a tube furnace under an ultrahigh pure nitrogen gas flow, and held for 2 h at the desired temperature. After cooling down to room temperature, the carbonized black samples were dried in vacuum for 24 h at 70 °C and denoted as FCDTPA-500, FCDTPA-700 and FCDTPA-900 according to the target temperature.

Synthesis of the potassium hydroxide activated carbon materials

The precursor of FCDTPA and KOH (1/4, mass ratio) were dispersed in a mixture solution of ethanol and water (95/5, v/v) and stirred overnight at room temperature. The resulting mixture was distilled to remove the solvents and the brown residue was dried in vacuum for 24 h at 70 °C. Carbonization of the FCDTPA/KOH mixture was carried out in a nickel crucible placed within a tube furnace by heating the sample to the target temperatures of 500, 700 and 900 °C with a heating rate of 2 °C min^{-1}, and held for 2 h at the desired temperature under an ultrahigh pure nitrogen gas flow. After cooling down to room temperature, the black residue was washed with 2 mol L^{-1} HCl to remove the excess KOH and salts, further purification of the activated carbon was carried out by washing with distilled water, ethanol and acetone, respectively. The resulting activated carbons were dried in vacuum for 24 h at 70 °C and denoted as FCDTPA-K-500, FCDTPA-K-700 and FCDTPA-K-900 according to the target temperature.

Characterization

The thermal properties of the precursor and all of the carbonized materials were evaluated using a thermogravimetric analysis (TGA) with a differential thermal analysis instrument (Q1000DSC + LNCS + FACS Q600SDT) over the temperature range from 30 to 1000 °C under a nitrogen atmosphere with a heating rate of 10 °C min^{-1}. Elemental analysis was carried out on a EURO EA3000 Elemental Analyzer. The FT-IR spectra were collected in transmission on a Tensor 27 FT-IR spectrometer (Bruker) using KBr disks. Raman spectra were carried out on an inVia Raman Microscope (Renishaw). Solid state magic angle spinning ^{13}C CP/MAS NMR measurement was carried out on a Bruker Avance III model 400 MHz NMR spectrometer at a MAS rate of 5 kHz. The morphology and energy dispersive X-ray spectroscopy (EDX) were carried out on an environmental scanning electron microscope (FEI, Quanta 200). Powder X-ray diffraction measurement was carried out on X-ray Deffractometer (D/Max-3c). Surface areas and pore size distributions were measured by nitrogen adsorption and desorption at 77.3 K using an ASAP 2420-4 (Micromeritics) volumetric adsorption analyzer. Samples were degassed at 120 °C (for the precursor) and 300 °C (for the carbonized materials) for 15 hours under vacuum (10^{-5} bar) before analysis. Gas sorption isotherms were measured on an ASAP 2420-4 as well.

Results and discussion

The precursor, a nitrogen-rich hypercrosslinked porous organic polymer network, was synthesized via facile Friedel-Crafts alkylation of DTPA using a formaldehyde dimethyl acetal crosslinker promoted by anhydrous FeCl$_3$ (Scheme 1).[28, 29] Carbonization was carried out by directly heating the precursor to the target temperatures of 500, 700 and 900 ^{0}C with/without potassium hydroxide activation before carbonization. All the carbonized materials are insoluble in conventional organic solvents and also chemically stable with aqueous solutions of acids and bases, such as HCl and NaOH. The precursor of FCDTPA shows less thermal stability as revealed by TGA (up to 300 ^{0}C, *Fig. S1*) compared with the carbonized materials, which could be attributed to the presence of cross-linker of methylene groups in the precursor which reduced the thermal stability. All of the carbonized materials show robust thermal stability up to 500 ^{0}C in nitrogen atmosphere, and the thermal stability increased along with the elevated temperature, indicating that the carbonization degree increased at high temperature. This is also evidenced by the microanalysis of the carbonized materials showing increased carbon content, while decreased nitrogen and hydrogen contents with the elevated temperature (*Table S1*). FT–IR spectra of the carbonized materials showed that the disappearance of C–H bands at 815 cm^{-1}, indicating that the elimination of hydrogen, and the peak at around 1500 cm^{-1} which is assigned to the C=C vibration bands from the benzene unit could not be observed for all of the carbonized materials (*Fig. S2*). The solid state ^{13}C CP/MAS NMR spectrum of the precursor of FCDTPA and the assignment of the resonances was shown in *Fig. S3*. No iron or potassium residue could be detected in the FCDTPA precursor or in the KOH activated carbonized materials by EDX after exhaustive purification (*Fig. S4*, *S5*). Electron microscopy images (SEM) showed that the carbonized materials consist of regular spherical small particles, and the particle size

become bigger and slight lamellar structure was also observed with elevated temperature (*Fig. S6, S7*), which could be explained by the carbonized degree enhancement at higher temperature. Powder X-ray diffraction measurements revealed that most of the carbonized materials were amorphous in nature, with the exception of FCDTPA-900, where some evidence for order was given based on the two diffraction peaks at 2θ values of around 25º and 43º, which can be assigned to 002 (25º) and 100 (43º) graphitic planes of carbon materials, respectively (*Fig. S8*),[30] indicating that the degree of graphitic nature for the carbon materials is improved at a higher temperature, which is in good agreement with the Raman spectra of the direct carbonization materials showing that the intensity of G band (around at 1593 cm^{-1}) from sp^2-bonded carbon atoms in graphite layer[31] increased along with the elevated temperature *(Fig. S9)*.
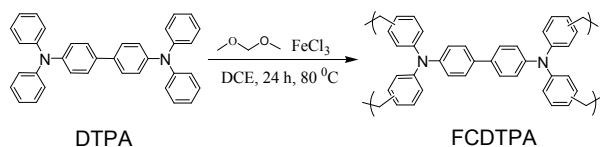
Scheme 1 Synthesis route to the precursor of FCDTPA.

Nitrogen sorption experiments were performed at 77.3 K to examine the surface area and the pore size distribution of the carbonized materials (Fig. 1a, 1b). All of the carbonized materials show Type–I nitrogen sorption isotherms with steep increases at low relative pressure ($P/P_0 < 0.001$), suggesting that micropores are dominant in the samples. A steep rise in the nitrogen adsorption isotherms for most of the carbonized materials, particularly for FCDTPA-500 and FCDTPA-K-900, was also observed at high relative pressures ($P/P_0 > 0.9$), indicating the presence of some mesopores and/or macropores in these carbonized materials as well, which are probably due to inter-particle porosity or void.[32] Significant hysteresis was observed for the precursor of FCDTPA, which is consistent with elastic deformations or swelling as a result of gas sorption.[33] As a sharp contrast, almost no hysteresis was observed for the carbonized materials, particularly for the KOH-activated carbonized materials, indicating that the rigidity of the framework increased

and almost no ''soft'' part remained after carbonization. Figure 1c & 1d show the pore size distribution (PSD) curves for the precursor and the carbonized materials as calculated using nonlocal density functional theory (NL-DFT). The precursor of FCDTPA exhibits a median micropore diameter of 0.97 nm with a shoulder peak around at 1.64 nm with a spot mesopores peaked at around 2.12 and 4.98 nm. After direct carbonization, the samples show narrower pore diameter centered at around 0.85 nm, and the intensity of the peak at 1.64 nm and the mesopore peaks decreased gradually along with the elevated temperature, especially the peak at around 1.64 nm almost could not be observed for FCDTPA-900 (Fig. 1c), indicating that much more micropores and uniform micropore size were produced at higher temperature. As for the KOH-activated carbonized materials, FCDTPA-K-500 shows the smallest pore size at 0.79 nm, while some new mesopores centered at 2.4 nm was observed for FCDTPA-K-900, which could be produced from the hard template effect of the adsorbed KOH (Fig. 1d).[17] The apparent BET surface area was found to be 871 m^2 g^{-1} for the FCDTPA precursor. After direct carbonization without KOH as an activating agent, the surface areas of FCDTPA samples decreased to the range from 417 to 520 m^2 g^{-1}, this could be explained by the collapse of the pores in the porous organic polymer during carbonization with elevated temperature. On contrast, the FCDTPA-K samples carbonized at high temperature (> 500 ^{0}C) with KOH as an activating agent show increased surface area (Table 1), which could be attributed to the CO_2 produced by the decomposition of K_2CO_3 generated in the activation process at high temperature contribute to the further development of porosity through the gasification of carbon.[25, 30] FCDTPA-K-700 shows the highest surface area of 2065 m^2 g^{-1} among the samples, which is significantly higher 2.4 times than that of the precursor. Compared with FCDTPA-K-700, however, FCDTPA-K-900 carbonized at 900 ^{0}C shows lower surface area, which is probably due to the collapse of the pores in the carbon material at higher temperature. These results demonstrate that both the carbonization temperature and KOH have big influence on the pore structure (pore size & surface area) of the carbonized materials.

Table 1 Summary of pore properties for the carbonized materials

Samples	S_{BET} [a]	S_{Micro} [b]	V_{Micro} [c]	V_{Total} [d]	S_{Micro}/S_{BET}	V_{Micro}/V_{Total}
	[m^2 g^{-1}]	[m^2 g^{-1}]	[cm^3 g^{-1}]	[cm^3 g^{-1}]	[%]	[%]
FCDTPA	871	667	0.33	0.66	76.57	50.00
FCDTPA-500	520	335	0.15	0.58	64.42	25.86
FCDTPA-700	417	341	0.16	0.31	81.77	51.61
FCDTPA-900	426	358	0.18	0.33	84.04	54.55
FCDTPA-K-500	749	660	0.29	0.47	88.12	61.70
FCDTPA-K-700	2065	1979	0.91	1.08	95.84	84.26
FCDTPA-K-900	1668	1119	0.49	1.09	67.08	44.95

[a] Surface area calculated from N_2 adsorption isotherm in the relative pressure (*P/Po*) range from 0.05 to 0.20; [b] Micropore surface area calculated from the N_2 adsorption isotherm using t-plot method based on the Harkins-Jura Equation; [c] The micropore volume derived from the t-plot method; [d] Total pore volume at *P/Po* = 0.98.

The high specific surface area and the microporous nature of the carbonized materials inspired us to investigate their gas uptake capacities. Hydrogen sorption isotherms of the carbonized materials at 77.3 K up to a pressure of 1.13 bar are shown in Fig. 2a & 2b. The three direct carbonization materials without KOH as an activating agent show lower hydrogen uptake abilities compared with the precursor of FCDTPA because of the decrease of surface area for these carbonized materials, which could be attributed to the pores collapsing during the process of carbonization. On contrast, all of the KOH-activated carbonized materials show enhanced hydrogen uptake abilities, particularly for FCDTPA-K-700 with the highest surface area showing the largest hydrogen uptake ability as high as 292 cm^3/g (~2.61 wt%) at 77.3 K / 1.13 bar because of its highest contents of micropore surface area and micropore volume among the samples (Table 1),

since micropores, not mesopores, mostly contribute to the H$_2$ adsorption at these pressures and temperatures.[34, 35] The hydrogen sorption of 2.61 wt% for FCDTPA-K-700 is comparable to or higher than that of some previously reported porous carbon materials under the same conditions, such as the YSN-1$_{400°C}$ (2.6 wt%, 77 K / 1.0 bar) carbonized from spirobifluorene-based porous organic polymer,[14] the PAF-1-380 (1.99 wt%, 77 K / 1.0 bar) carbonized from PAF-1,[16] the activated carbons of AC1 (1/4-700) (2.5 wt%, 77 K / 1.0 bar) derived from cellulose,[25] and the nanoporous carbon of C1000 (2.77 wt%, 77 K / 1.0 bar) produced from the metal-organic framework of ZIF-8,[36] but lower than the K-PAF-1-750 (3.06 wt%, 77 K / 1.0 bar) carbonized from the KOH-activated PAF-1,[17] and the MDC-1 (3.25 wt%, 77 K / 1.0 bar) carbonized from highly crystalline metal-organic frameworks.[15]
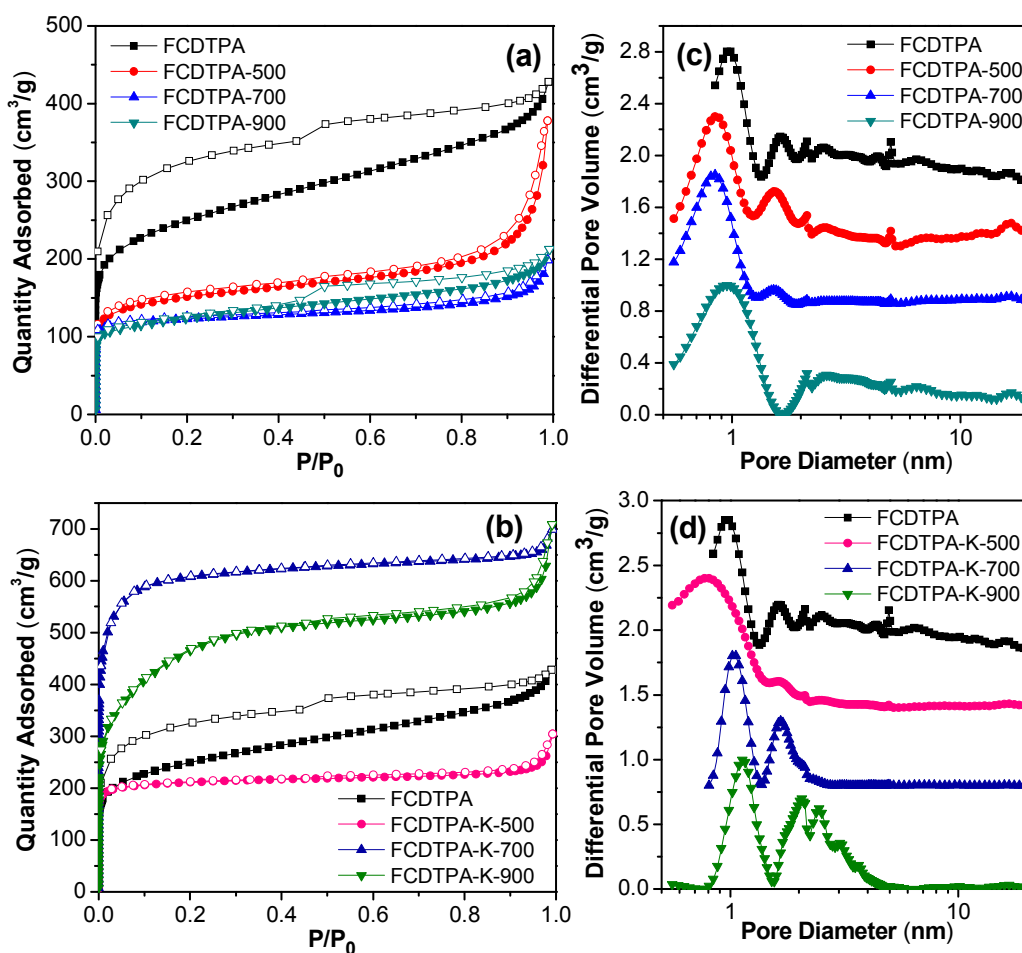
Fig. 1 Nitrogen adsorption/desorption isotherms for (a) the direct carbonized materials, and (b) the activated carbon materials (the adsorption branch is labeled with filled symbols and the desorption branch is labeled with open symbols); Pore size distribution curves calculated by NL-DFT for (c) the direct carbonized materials , and (d) the activated carbon materials.

The CO$_2$ uptakes of the carbon materials were measured up to 1.13 bar at 273 K (Fig. 2c, 2d). Most of the carbonized materials without KOH as an activating agent show decreased CO$_2$ uptake ability compared with the precursor of FCDTPA, which could be

partially attributed to the decrease of surface area after directly carbonization, while FCDTPA-700 shows a puny enhancement in CO$_2$ uptake (2.92 mmol g^{-1} at 273 K / 1.13 bar) compared with the precursor (2.82 mmol g^{-1} at 273 K / 1.13 bar) although it has

lower surface area, this could be explained by the fact that almost all of the pores in FCDTPA-700 are micropores and the pore sizes are less than 1 nm, which is preferred to adsorb CO_2 molecules.[37] On the contrary, all of the KOH-activated carbon materials show a significant improvement for CO_2 uptake, particularly for FCDTPA-K-700 with the highest surface area showing the highest CO_2 uptake ability of 6.51 mmol g^{-1} at 1.13 bar and 273 K. Furthermore, no saturation is achieved in the 1.13 bar pressure range (Fig. 2d), which suggests that a higher CO_2 capacity could be achieved by increasing the pressure above 1.13 bar. The superior CO_2 uptake ability for FCDTPA-K-700 could be attributed to its higher microporous surface area, micropore volume and relative high nitrogen content. The CO_2 uptake ability of 6.51 mmol g^{-1} for FCDTPA-K-700 lies towards the upper end when compared to other carbon materials under the same conditions, such as the carbon spheres of CS3-6A (6.2 mmol g^{-1}) obtained by sol-gel method,[24] the SC-800-A (6.7 mmol g^{-1}) carbonized from Saran polymer,[38] the PAF-1-450 (4.5 mmol g^{-1}) carbonized from PAF-1,[16] and the K-PAF-1-600 activated carbon (7.2 mmol g^{-1}).[17] It is also higher than most of N-doped carbon materials under the same conditions, such as the NPC-650 (5.26 mmol g^{-1}) carbonized from porous polyimine,[22] the NC-900 (5.1 mmol g^{-1}) carbonized from N-decorated ZIF-8,[23] the N-doped nanocomposite Zn/Ni-ZIF-8-1000 (4.25 mmol g^{-1}),[39] and the nitrogen enriched porous carbon spheres (6.2 mmol g^{-1}).[24]

Table 2 Gas uptakes for the carbonized materials

Polymer	H$_2$ uptake [a] [wt%]	CH$_4$ uptake [b] [mmol g^{-1}]	CO$_2$ uptake [b] [mmol g^{-1}]	CO$_2$ uptake [c] [mmol g^{-1}]	Selectivity [d]	
					CO$_2$/CH$_4$	CO$_2$/N$_2$
FCDTPA	1.52	0.89	2.83	1.51	5.2	30.3
FCDTPA-500	0.82	0.82	2.11	1.40	7.6	57.9
FCDTPA-700	1.09	1.39	2.92	2.15	5.0	36.3
FCDTPA-900	1.43	1.19	2.70	1.79	5.3	34.1
FCDTPA-K-500	1.65	1.76	4.53	3.18	8.0	53.5
FCDTPA-K-700	2.61	2.36	6.51	3.71	4.0	19.6
FCDTPA-K-900	1.72	1.28	3.41	1.95	3.4	6.1

[a] Data were obtained at 1.13 bar and 77.3 K; [b] Data were obtained at 1.13 bar and 273 K; [c] Data were obtained at 1.13 bar and 298 K; [d] Adsorption selectivity based on the Henry law.

To determine the binding affinity of the carbonized materials for CO_2, the isosteric heat of adsorption (Q_{st}) was calculated from the Clausius–Clapeyron equation using the CO_2 adsorption data collected at 273 K and 298 K, respectively (*Fig. S11*). The precursor of FCDTPA shows the isosteric heat of CO_2 adsorption of 30.55 kJ mol^{-1} at zero coverage because of its high nitrogen content. After direct carbonization, the samples of FCDTPA-500 and FCDTPA-700 show a little decrease in Q_{st}, which could be attributed to the decrease of nitrogen content, while FCDTPA-900 shows a little enhanced in Q_{st} (31.22 kJ mol^{-1}) due to its high contents of micropore surface area and micropore volume as discussed above. As for the KOH-activated carbon materials, the FCDTPA-K-500 sample shows the highest Q_{st} (30.97 kJ mol^{-1}) among the samples, which could be attributed to the smaller micropore size of 0.79 nm, and small pore sizes known to increase the heat of adsorption.[40] However, as the lower surface area and pore volume, FCDTPA-K-500 shows less CO_2 adsorption (4.53 mmol g^{-1} at 273 K / 1.13 bar) than FCDTPA-K-700. It is worth noting that most of the Q_{st} for the carbonized materials can remain nearly constant over a wide range of CO_2 loading, particularly for FCDTPA-700 and FCDTPA-K-700, which suggests that a significantly higher CO_2 uptake could probably be achieved by increasing the micropore surface area and micropore volumes of the adsorbent–indeed, FCDTPA-K-700 with the highest surface area shows the largest CO_2 uptake capacity of 6.51 mmol g^{-1} at 273 K up to 1.13 bar.

The methane sorption performance of the carbon materials was also explored (Fig. 2e, 2f). As expected, the activated carbon materials show significant enhanced methane uptakes compared with the precursor, especially for FCDTPA-K-700 with the highest surface area (2065 m^2 g^{-1}) and micropore volume (0.91 cm^3 g^{-1}) exhibits the largest methane uptake ability of 2.36 mmol g^{-1} at 273 K / 1.13 bar (Table 2). This value is comparable to the activated carbon of K-PAF-1-600 (2.4 mmol g^{-1} at 273 K / 1.0 bar) produced from PAF-1,[17] the poly (vinylidene chloride)-based carbon of PC (2.05 mmol g^{-1} at 298 K / 1.0 bar),[41] and higher than the PAF-1-450 (1.41 mmol g^{-1} at 273 K / 1.0 bar).[16] In order to investigate the gas adsorption selectivity of the carbon materials, CO_2, N_2, and CH_4 sorption properties were measured by volumetric methods at the same conditions (*Fig. S12–18*). The selectivity was estimated using the ratios of the Henry law constant calculated from the initial slopes of the single-component gas adsorption isotherms at low pressure coverage (< 0.15 bar) and the results were summarized in Table 2. It was found that both the CO_2/CH_4 and CO_2/N_2 adsorption selectivity for the carbonized materials decreased with the elevated temperature. For example, the FCDTPA-500 shows the highest CO_2/N_2 adsorption selectivity of 57.9 among the three direct carbonized materials, and FCDTPA-K-500 shows the highest CO_2/N_2 adsorption selectivity of 53.5 among the three KOH-activated carbonized materials, which could be attributed to the relative higher nitrogen content and the smaller micropore size in

these samples carbonized under lower temperature. FCDTPA-K-900 shows the lowest CO_2/N_2 adsorption selectivity of 6.1 among the carbonized materials because it has the lowest nitrogen content and also has much more mesopores as evidenced by the microanalysis and the pore size distribution discussed above. These results prove that, besides the specific surface area, the

micropore size and the nitrogen content in the porous carbon also play crucial roles in CO_2/N_2 adsorption selectivity. Therefore, one could expect to obtain enhanced CO_2/N_2 adsorption selectivity by either tuning the micropore size or introducing high nitrogen content into the carbon materials.
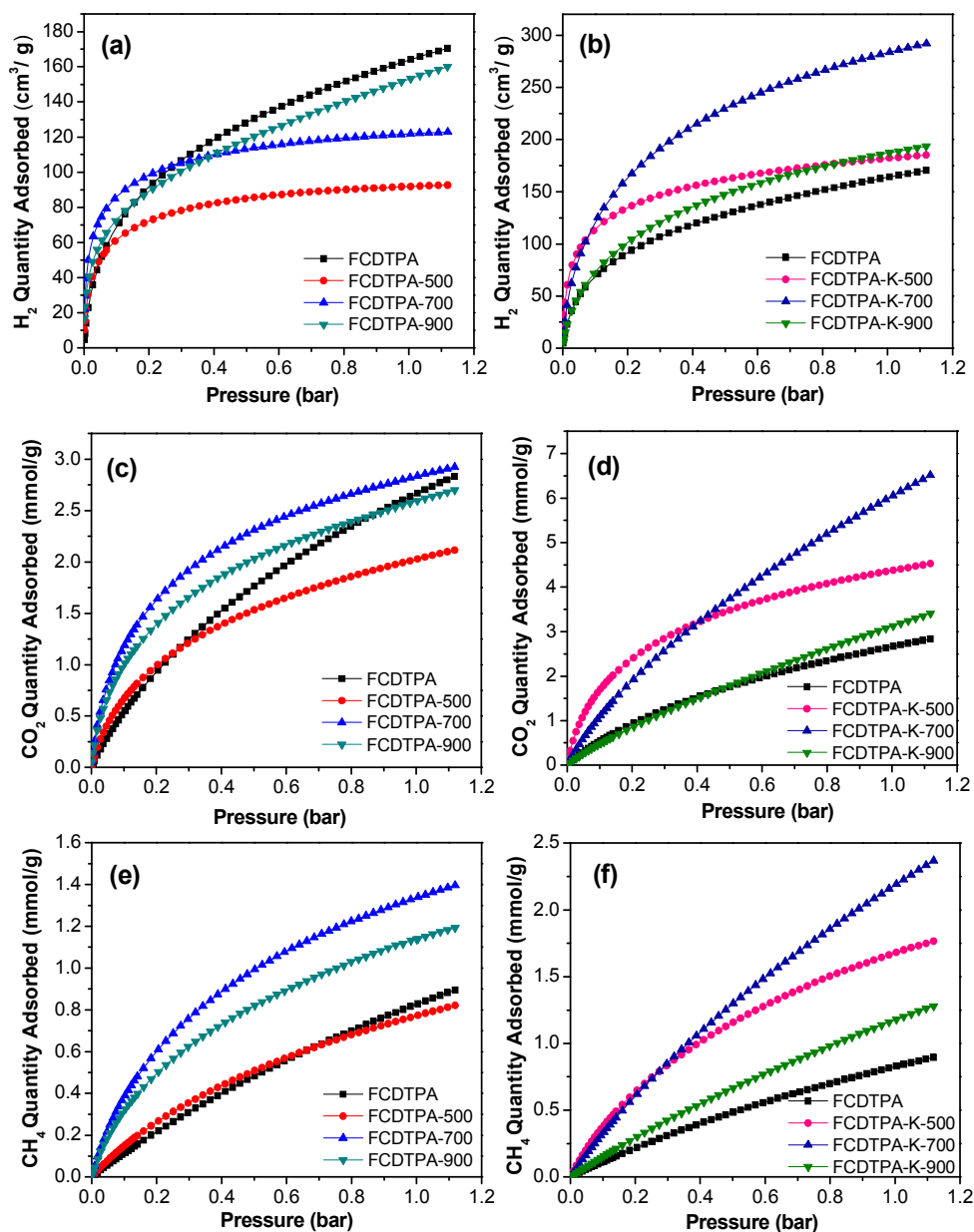
Fig. 2 Volumetric H_2 sorption curves for the carbonized materials at 77.3 K up to 1.13 bar (a-b); CO_2 adsorption isotherms for the carbonized materials at 273 K up to 1.13 bar (c-d); CH_4 adsorption isotherms for the carbonized materials at 273 K up to 1.13 bar (e-f).

Conclusion

In summary, a series of carbonized materials was obtained using nitrogen-rich hypercrosslinked porous organic polymer as the precursor by high-temperature treatment with/without potassium hydroxide activation. Both of the carbonization temperature and hydroxide activation. Both of the carbonization temperature and

the chemical activation agent of potassium hydroxide have big influence on the pore structure (pore size & surface area) of the carbonized materials. The potassium hydroxide activated carbons show high surface areas and enhanced gas uptake abilities. The activated carbon material of FCDTPA-K-700 exhibits a high surface area of 2065 m² g⁻¹ and an exceptionally high carbon

dioxide uptake up to 6.51 mmol g^{-1} (1.13 bar / 273 K), and with the H$_2$ and CH$_4$ uptake abilities of 2.61 wt% (1.13 bar / 77.3 K) and 2.36 mmol g^{-1} (1.13 bar / 273 K), respectively. Given the high surface areas, the outstanding gas sorption performances, and the facile preparation strategy, these novel carbon materials are very promising for industrial applications such as carbon dioxide capture and high-density clean energy storage.

Acknowledgements

Notes and references

School of Materials Science and Engineering, Shaanxi Normal University, Xi'an, 710062, Shaanxi, P. R. China.
E-mail: jiaxing@snnu.edu.cn

†Electronic Supplementary Information (ESI) available: Elemental analysis, TGA, FT-IR, Raman spectra, Solid state ^{13}C NMR, SEM, PXRD, isosteric heat of CO$_2$ adsorption and the gas adsorption. See DOI: 10.1039/b000000x/

1. P. Markewitz, W. Kuckshinrichs, W. Leitner, J. Linssen, P. Zapp, R. Bongartz, A. Schreiber and T. E. Müller, *Energy Environ. Sci.*, 2012, **5**, 7281.

2. R. Dawson, E. Stöckel, J. R. Holst, D. J. Adams and A. I. Cooper, *Energy Environ. Sci.*, 2011, **4**, 4239.

3. Z. Xiang and D. Cao, *J. Mater. Chem. A*, 2013, **1**, 2691.

4. Y. Xu, S. Jin, H. Xu, A. Nagai and D. Jiang, *Chem. Soc. Rev.*, 2013, **42**, 8012.

5. D. Wu, F. Xu, B. Sun, R. Fu, H. He and K. Matyjaszewski, *Chem. Rev.*, 2012, **112**, 3959.

6. R. V. Siriwardane, M.-S. Shen and E. P. Fisher, *Energy Fuels*, 2003, **17**, 571.

7. K. Sumida, D. L. Rogow, J. A. Mason, T. M. McDonald, E. D. Bloch, Z. R. Herm, T. H. Bae and J. R. Long, *Chem. Rev.*, 2012, **112**, 724.

8. Y. Jin, B. A. Voss, A. Jin, H. Long, R. D. Noble and W. Zhang, *J. Am. Chem. Soc.*, 2011, **133**, 6650.

9. T. Tozawa, J. T. A. Jones, S. I. Swamy, S. Jiang, D. J. Adams, S. Shakespeare, R. Clowes, D. Bradshaw, T. Hasell, S. Y. Chong, C. Tang, S. Thompson, J. Parker, A. Trewin, J. Bacsa, A. M. Z. Slawin, A. Steiner and A. I. Cooper, *Nat. Mater.*, 2009, **8**, 973.

10. R. Dawson, A. I. Cooper and D. J. Adams, *Prog. Polym. Sci.*, 2012, **37**, 530.

11. S.-Y. Ding and W. Wang, *Chem. Soc. Rev.*, 2013, **42**, 548.

12. J. Lee, J. Kim and T. Hyeon, *Adv. Mater.*, 2006, **18**, 2073.

13. Y. Xia, Z. Yang and Y. Zhu, *J. Mater. Chem. A*, 2013, **1**, 9365.

14. B. G. Hauser, O. K. Farha, J. Exley and J. T. Hupp, *Chem. Mater.*, 2013, **25**, 12.

15. S. J. Yang, T. Kim, J. H. Im, Y. S. Kim, K. Lee, H. Jung and C. R. Park, *Chem. Mater.*, 2012, **24**, 464.

16. T. Ben, Y. Li, L. Zhu, D. Zhang, D. Cao, Z. Xiang, X. Yao and S. Qiu, *Energy Environ. Sci.*, 2012, **5**, 8370.

17. Y. Li, T. Ben, B. Zhang, Y. Fu and S. Qiu, *Sci. Rep.*, 2013, **3**, 2420.

18. Y. Zhang, B. Li, K. Williams, W. Y. Gao and S. Ma, *Chem. Commun.*, 2013, **49**, 10269.

19. X. Jin, V. V. Balasubramanian, S. T. Selvan, D. P. Sawant, M. A. Chari, G. Q. Lu and A. Vinu, *Angew. Chem. Int. Ed.*, 2009, **48**, 7884.

20. K. Gong, F. Du, Z. Xia, M. Durstock and L. Dai, *Science*, 2009, **323**, 760.

21. L. Wang and R. T. Yang, *J. Phys. Chem. C*, 2012, **116**, 1099.

22. J. Wang, I. Senkovska, M. Oschatz, M. R. Lohe, L. Borchardt, A. Heerwig, Q. Liu and S. Kaskel, *J. Mater. Chem. A*, 2013, **1**, 10951.

23. A. Aijaz, N. Fujiwara and Q. Xu, *J. Am. Chem. Soc.*, 2014, **136**, 6790.

24. N. P. Wickramaratne, J. Xu, M. Wang, L. Zhu, L. Dai and M. Jaroniec, *Chem. Mater.*, 2014, **26**, 2820.

25. M. Sevilla, A. B. Fuertes and R. Mokaya, *Energy Environ. Sci.*, 2011, **4**, 1400.

26. X. Yang, S. Yao, M. Yu and J.-X. Jiang, *Macromol. Rapid Commun.*, 2014, **35**, 834.

27. W. Z. Yuan, P. Lu, S. Chen, J. W. Lam, Z. Wang, Y. Liu, H. S. Kwok, Y. Ma and B. Z. Tang, *Adv. Mater.*, 2010, **22**, 2159.

28. B. Li, R. Gong, W. Wang, X. Huang, W. Zhang, H. Li, C. Hu and B. Tan, *Macromolecules*, 2011, **44**, 2410.

29. S. Yao, X. Yang, M. Yu, Y. Zhang and J.-X. Jiang, *J. Mater. Chem. A*, 2014, **2**, 8054.

30. G. Srinivas, J. Burress and T. Yildirim, *Energy Environ. Sci.*, 2012, **5**, 6453.

31. W. Ren, F. Li, P. Tan and H.-M. Cheng, *Phys. Rev. B*, 2006, **73**, 115430.

32. J. Weber, J. Schmidt, A. Thomas and W. Bohlmann, *Langmuir*, 2010, **26**, 15650.

33. J. Weber, M. Antonietti and A. Thomas, *Macromolecules*, 2008, **41**, 2880.

34. J.-X. Jiang, A. Laybourn, R. Clowes, Y. Z. Khimyak, J. Bacsa, S. J. Higgins, D. J. Adams and A. I. Cooper, *Macromolecules*, 2010, **43**, 7577.

35. J. X. Jiang, F. Su, H. Niu, C. D. Wood, N. L. Campbell, Y. Z. Khimyak and A. I. Cooper, *Chem. Commun.*, 2008, 486.

36. H. L. Jiang, B. Liu, Y. Q. Lan, K. Kuratani, T. Akita, H. Shioyama, F. Zong and Q. Xu, *J. Am. Chem. Soc.*, 2011, **133**, 11854.

37. T. Ben, H. Ren, S. Ma, D. Cao, J. Lan, X. Jing, W. Wang, J. Xu, F. Deng, J. M. Simmons, S. Qiu and G. Zhu, *Angew. Chem. Int. Ed.*, 2009, **48**, 9457.

38. A. Dziura, M. Marszewski, J. Choma, L. K. C. de Souza, Ł. Osuchowski and M. Jaroniec, *Ind. Eng. Chem. Res.*, 2014, DOI: 10.1021/ie5004448.

39. R. Li, X. Ren, X. Feng, X. Li, C. Hu and B. Wang, *Chem. Commun.*, 2014. DOI: 10.1039/c4cc01087f.

40. J. Germain, J. M. Frechet and F. Svec, *Small*, 2009, **5**, 1098.

41. J. Cai, J. Qi, C. Yang and X. Zhao, *ACS Appl. Mater. Interfaces*, 2014, **6**, 3703.

ARTICLE TYPE

Table of Content

Carbonized materials form a nitrogen-rich hypercrosslinked porous organic polymer exhibit a high surface area of 2065 m^2 g^{-1} and an exceptionally high carbon dioxide uptake up to 6.51 mmol g^{-1} (1.13 bar / 273 K).

5

10
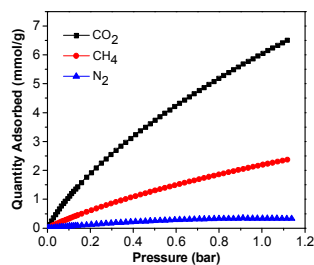
Xiao Yang, Miao Yu, Yang Zhao, Chong Zhang, Xiaoyan Wang, Jia-Xing Jiang*

15 **Remarkable Gas Adsorption by Carbonized Nitrogen-Rich Hypercrosslinked Porous Organic Polymers**